49th AIAA Aerospace Sciences Meeting including the New Horizons Forum and Aerospace Exposition
4 - 7 January 2011, Orlando, Florida

AIAA 2011-958

On Multi-Barrier Plasma Actuators

Ryan Durscher[*] and Subrata Roy[†]

Computational Plasma Dynamics Laboratory and Test Facility, Applied Physics Research Group
Mechanical and Aerospace Engineering Department
University of Florida, Gainesville, FL 32611-6300

The multi-barrier plasma actuator (MBPA) is an extension on the standard dielectric barrier discharge (DBD) actuator which consists of conducting electrodes placed asymmetrically on a single dielectric substrate. The MBPA design incorporates multiple dielectric layers and phase lagged powered electrodes into the standard design in an effort to create a stronger discharge. The results of this increase could lead to higher induced velocities/resultant forces. In a prior study, the MBPA design was found to outperform the standard actuator in both measured force and effectiveness (ratio of the induced force over consumed power). The present investigation is an extension on this previous work to expound upon the broad design space of the multi-barrier configuration. The resultant force produced by both bi-layer and tri-layer actuators are measured directly using a precision force balance. The results of these experiments are then compared with the standard actuator design. In addition, the influence of mixing dielectric materials is also explored. For all test cases the total power delivered to the actuator is calculated and presented.

Nomenclature

f = measured thrust, mN
I = instantaneous applied input current, A
l = length of electrode, mm
L_g = width of grounded electrode for bi-layer configuration, mm
P_{tot} = total power delivered to the actuator, W
t = thickness of dielectric substrate, mm
V = instantaneous applied input voltage, kV
w = width of electrode, mm
β = relative phase angle
ε = relative dielectric constant
γ = effectiveness, mN/W
ϕ = peak applied potential, kV
ω = reference phase angle of driving potential

I. Introduction

The aerodynamic benefits of a single dielectric barrier plasma actuator at or near atmospheric pressures have been widely documented in the last one and a half decades.[1-5] The actuator design most readily investigated consists of asymmetric conducting electrodes placed on a dielectric substrate. In the conventional arrangement one electrode (exposed to the surrounding gas) is supplied with a high voltage AC signal while the lower electrode (which is typically embedded in the dielectric) remains grounded. When the electric field reaches sufficient strength the air becomes weakly ionized in the vicinity of the exposed electrode resulting in a dielectric barrier discharge (DBD). The presence of the plasma leads to a momentum coupling with the surrounding neutrally charged air which manifests itself as a primarily tangential wall jet.

Varying aspects of this conventional design such as electrode geometry, input voltage, dielectric material, electrode spacing, voltage waveform, and driving frequency have been investigated by numerous authors.[1-9] A recent annual review by Corke et al. provides a brief overview of these efforts and current attempts to combine them into

---

[*] Graduate Student, Student Member AIAA, dursch@ufl.edu
[†] Associate Professor, Associate Fellow AIAA, roy@ufl.edu

an optimized device.[10] Although these efforts have provided improved operation as well as a great deal of insight into the operational mechanisms of the DBD plasma actuator, there is still a need for higher performance. In an attempt to meet this need the concept of multi-barrier plasma actuators (MBPA) was presented in a patent by Roy.[11] The MBPA is an extension on the single layer asymmetric geometry described above to include additional dielectric layers and powered electrodes kept at phase differences (figure 1). Such a configuration opens up additional parameters to the DBD actuator design space. For example, as stated above numerous authors have looked at the influence that different dielectrics have on performance.[6, 9] The MBPA configuration goes a step beyond this point such that different materials may be combined into a single actuator Also, the vertical arrangement of electrodes and the influence of relative phase difference can be explored. Preliminary results on these multi layer configurations previously indicated[12] that the multi-barrier designs were capable of achieving higher resultant thrusts than what was considered the standard actuator configuration. The effectiveness, γ, which is a ratio of measured thrust to consumed power, was also found to improve. This paper is a documentation of this exploration of the MBPA design space. Using a direct force balance the resultant thrust from both bi-layer and tri-layer designs are measured and compared with the standard actuator. The influence of mixing two different dielectric materials into a single actuator is also addressed. For each configuration the total consumed power and the effectiveness is calculated and compared against the standard design.
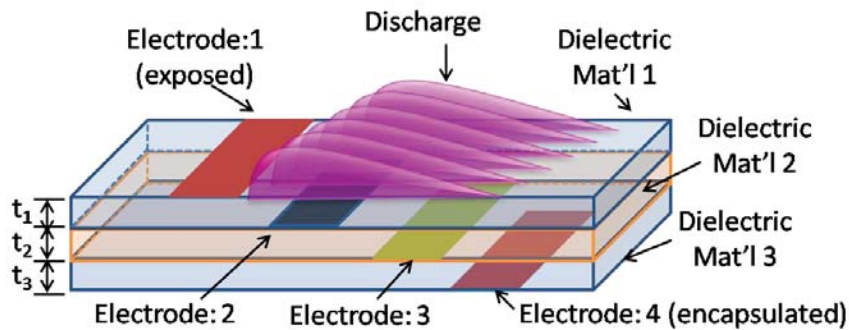

Figure 1. Tri-layer multi-barrier plasma actuator (MBPA) schematic.

II. Experimental Setup

A. Actuator designs

A general schematic of the electrode configurations used in this work are shown in figure 2. The standard DBD design, a bi-layer configuration, and tri-layer layout are represented by a, b, and c respectively. One will note that the overall thickness, t, of the combined dielectric materials remains the same between the different cases. This experimental configuration is different from reported preliminary results[12] in which the dielectric layers of unequal thickness were added as opposed to currently being split with equal thickness. The overall thickness, t, of the actuators investigated, with the exception of the mixed dielectric cases, was 6 mm. Similarly the horizontal footprint also remains the same between the configurations at $3w$, where w corresponds to the exposed electrode's width, 5 mm. For all three designs the exposed (top) electrode is powered with
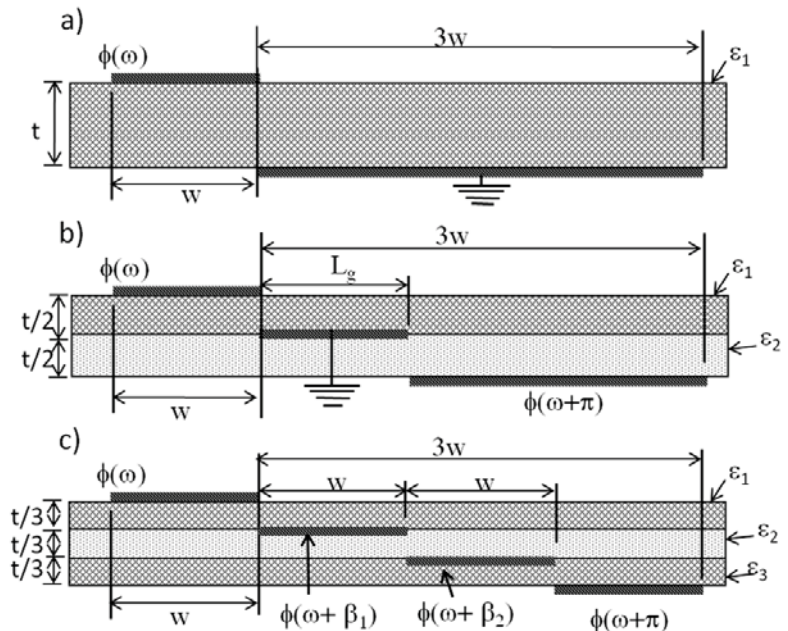

Figure 2. Schematic of actuator designs tested: a) standard actuator design, b) bi-layer MBPA, and c) tri-layer MBPA.

a peak potential, ϕ, at some reference phase angle of ω. As described previously the lower electrode for the standard actuator design is grounded. For the multi-barrier cases (figures 2b and 2c) the additional electrodes are also supplied with a potential ϕ, but are now temporally shifted by some phase angle β relative to the exposed electrode. In the current notation a positive β refers to a leading phase angle while negative values are considered lagging.

The electrodes in the designs are constructed from adhesively backed copper tape with a thickness of 70 μm. In all configurations the electrodes had a length, l, of 120.0 mm. The dielectric substrate used (again with the exception of the mixed dielectric cases) was acrylic. The layers of the multi-barrier actuators are held together using a two part epoxy. The epoxy layers were found to have thicknesses varying from 60-150 μm depending on the actuator. It is assumed, however, that the epoxy has a negligible influence on the plasma formation due to its relatively small thickness.

B. Discharge generation

As previously discussed the mulit-barrier plasma actuator requires multiple high voltage, AC signals in which the relative phase angles between the signals can be precisely controlled/manipulated. For the single and bi-layer actuators such signals originated from a dual output function generator (Tektronix AFG 3022B), where an 8 channel analog output PCI card (NI PCI-6713) and a LabVIEW interface was used for the tri-layer configuration. The low voltage sinusoidal waveforms at a driving frequency of 14 kHz were further amplified by dual channel audio amplifiers (QSC RMX 2450). The high voltage required to achieve a breakdown of the surrounding air was finally reached using a Corona Magnetics, Inc. high-voltage transformer. An example circuit configuration used to drive a tri-layer MBPA is shown in figure 3.
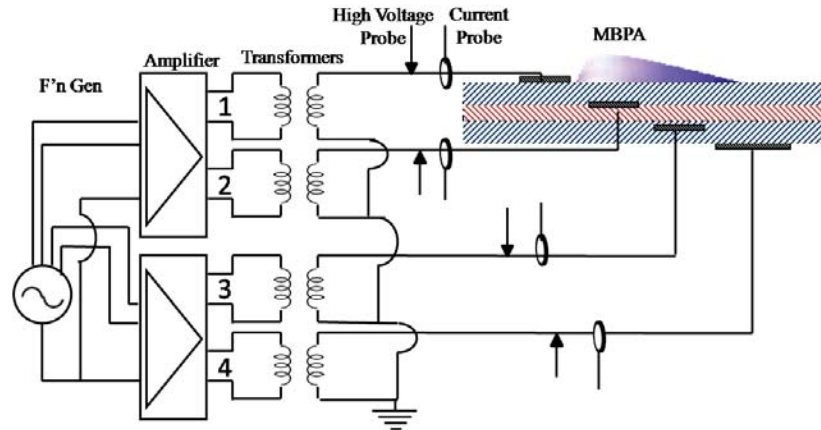
Figure 3. Circuit schematic used to generate a DBD discharge for a tri-layer multi-barrier plasma actuator.

As shown in the above diagram the voltage and current flowing through each branch in the circuit was monitored using high voltage and current probes. The voltage probes used were Tektronix's P6015A while Pearson Electronic's 2100 and Bergoz's CT-F1.0-B measured the current. Note that the primary difference between the two different ammeters was their respective bandwidth limits which had corresponding upper limits of 20 MHz and 100 MHz. For simplicity a 20 MHz bandwidth limit was set on the digitizing oscilloscopes regardless of which current probe was used. The oscilloscopes used to capture the voltage and current waveforms were Tektronix's DPO3014 and DPO2014. In a single acquisition the oscilloscopes captured 1 million points for each waveform at a sampling rate of 250 MSa/s.

For each input voltage for the standard and bi-layer configurations, 10 acquisitions were recorded which corresponds to 560 periods over which the calculated power is averaged. Conversely, due to the large amount of data downloaded, only 2 acquisitions (112 periods) were recorded for the tri-layer actuators. The total power, P_{tot}, delivered to the plasma actuator was considered to be a linear combination of the measured power flowing through each branch of the circuit (referring to figure 3). For example, the standard actuator has 1 branch, the bi-layer has 2, and the tri-layer has 4. The power delivered in each branch of the circuit was calculated based on summing the product of the instantaneous voltage, V, and current, I, and then dividing by the total number of acquired points. Equation 1 provides a representative equation used to determine the power for a tri-layer MBPA as shown in figure 3.

$$P_{tot} = \frac{1}{N}\left(\sum_{i=1}^{N}V_{i,1}I_{i,1} + \sum_{i=1}^{N}V_{i,2}I_{i,2} + \sum_{i=1}^{N}V_{i,3}I_{i,3} + \sum_{i=1}^{N}V_{i,4}I_{i,4}\right) \qquad (1)$$

C. Direct force measurement

The influence of the DBD plasma actuator in quiescent air is typically measured by two figures of merit: the peak velocity induced and the average resultant thrust. Here we focus on the experimental setup to measure the resultant thrust, f (figure 4). The thrust produced by the plasma actuators was measured directly using an Ohaus precision balance (Adventurer™ Pro AV313C) which has a resolution of 1 mg. The actuator was mounted to the scale via an acrylic stand which protruded through a small opening in the Faraday's cage. The purpose of the cage is to shield the balance from the electromagnetic noise present due to the high electric fields required to generate the plasma discharge. Due to the scale's high sensitivity, the slightest ambient room currents were found to significantly affect the measured resultant thrust. To resolve this issue the setup was housed in a large quiescent chamber with dimensions 0.61 m x 0.61 m x 1.22 m (width x depth x height). High voltage leads were connected to the actuator with 34 AWG magnetic wires in order to prevent wire droop from influencing the reading. Additional information regarding this setup may be found in reference 12.
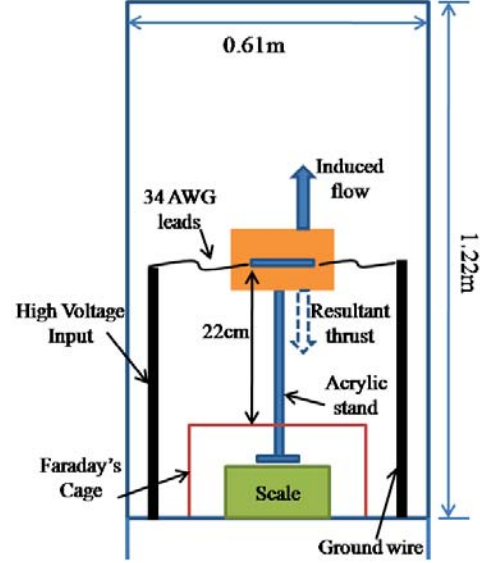

Figure 4. Experimental setup for direct force measurements of a DBD plasma actuator.

III. Results

A. Effect of L_g

As previously depicted in figure 2b the bi-layer MBPA consists of a middle grounded electrode sandwiched between two insulating dielectrics. The other two (powered) electrodes are then placed asymmetrically on the top and bottom of the dielectric sandwich. For this configuration the width, L_g, of the grounded electrode would argumentatively have a significant influence on the discharge and thus the resultant force. To investigate this influence, three different lengths corresponding to 3, 5, and 10 mm were evaluated. The results from the force measurements are presented in figure 5a plotted against the total voltage. The total voltage is the total potential supplied across the two powered electrodes on the actuator. For example, in these experiments the exposed (upper) and encapsulated (lower) electrodes are supplied with the same sinusoidal potential but with an 180° (previously shown to be an optimum operating point[12]) relative phase shift. Therefore, if a 7 kV$_{peak}$ voltage is applied to the two electrodes the peak total voltage across the actuator would be 14 kV$_{peak}$.

The measurements indicate that the resultant force for a given total voltage increases as the gap between the two electrodes approaches zero ($L_g \rightarrow 0$). This may be due to the modification of the electric field and consequently the force on the ions. As L_g is decreased from 10 to 3 mm the presence of the lower electrode can only increase the local electric field due to the 180° phase shift on the encapsulated electrode. It is important to note that the difference in measured force between L_g equal to 3 mm and 5 mm is small relative to the difference between either or with L_g equal to 10 mm. Also, if L_g was allowed to be zero one would simply end up with a dual powered standard actuator. However, when power consumption is taken into account, the actuator's effectiveness ($\gamma = f/P_{tot}$) is maximized for a grounded electrode length around 5 mm (figure 5b).
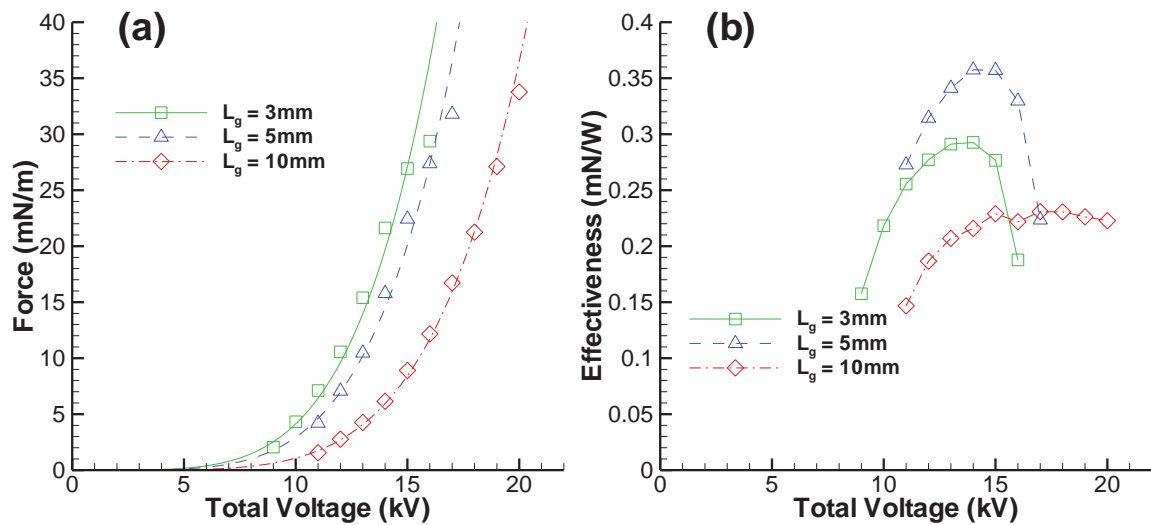
Figure 5. Influence of grounded electrode for a bi-layer configuration: a) force and b) effectiveness versus total voltage, respectively.

B. Influence of the grounded electrode for the bi-layer MBPA configuration

Although not shown, if one plots the data found in figure 5a as force versus electrode width for a constant voltage the resulting picture is similar to the findings of Forte et. al.[6]. In this prior investigation the influence of electrode spacing on the peak velocity produced by a mono-layer DBD actuator was appraised. Forte et. al. found that the induced velocity reaches a maximum for a gap spacing of 5 mm, but decreases rapidly if the electrode gap is further increased. With that in mind it is logical to speculate that the middle electrode (grounded) in the bi-layer configuration may not be playing a significant role and that by changing its length one is really only affecting the relative gap spacing between the exposed and encapsulated electrodes.

To further investigate this influence or importance, actuators were constructed without a middle grounded electrode, but were still dual powered. It was found that the middle electrode played no significant role in terms of force production or total power consumption (figure 6 and 8). It did, however, have an influence on the power distribution supplied to the two (upper and lower) electrodes. When the middle electrode was present, the upper (or exposed) electrode consumed significantly more power than the lower (or encapsulated) electrode. In this case 80-95% of the total power consumed by the device was supplied to the exposed electrode. Conversely, when removed, the consumed power between the upper and lower electrodes was approximately equal.

Such a result is not surprising when one considers the electric field lines of such arrangements (figure 7). For the case in which the grounded electrode is not present, the field lines will be drawn solely from the exposed electrode to the encapsulated powered electrode (figure 7a). The direction of the field lines would obviously be dependent on which part to the AC signal one is talking about, but as a result the work

Figure 6. Influence of the grounded electrode in the bi-layer MBPA configuration on force production.

done by each power supply should be roughly equally distributed between the two since each electrode should contribute to the ionization process. Conversely, when the grounded electrode is present an alternative path way or "stepping stone" is provided (figure 7b). The field lines for this configuration stemming from the exposed electrode
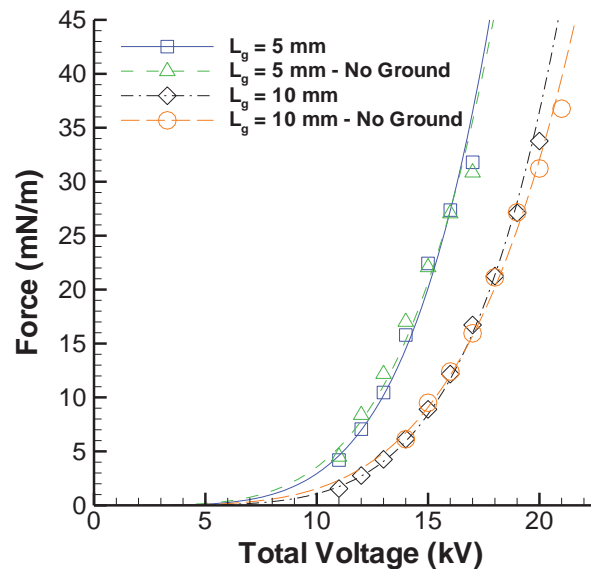
5
American Institute of Aeronautics and Astronautics

may terminate at the grounded electrode or, if the potentials are high enough, may stretch to the powered encapsulated electrode. This is schematically shown in figure7b and 7c in which ϕ_1 is greater than ϕ_2. In the first case the potential on the lower electrode is low enough that it virtually does not exist and contributes little to nothing to the plasma formation. That part of the circuit should then act as an ideal capacitor consuming little to no power. However, as the supplied potential is increased the presence of the lower electrode is seen and it begins contributing to the ionization process and thus the total power consumed by the actuator. These trends are found in the experimental data shown in figures 8a and 8b for a bi-layer MBPA with and without a grounded electrode. For low values of total voltage the power used by the encapsulated electrode when the grounded electrode is present is approximately zero, but begins to increase has the potential is increased.
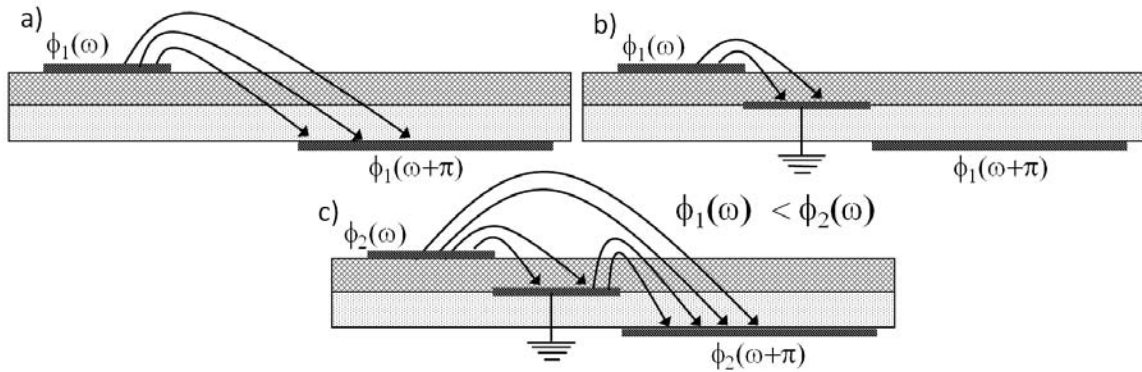
Figure 7. Schematic representation of the electric field lines for a bi-layer MBPA with and without a middle grounded electrode. a) No grounded electrode is present, b) grounded electrode is present but supplied potential is low, and c) grounded electrode is present and supplied potential is of sufficient strength that the exposed electrode sees the presence of the encapsulated.
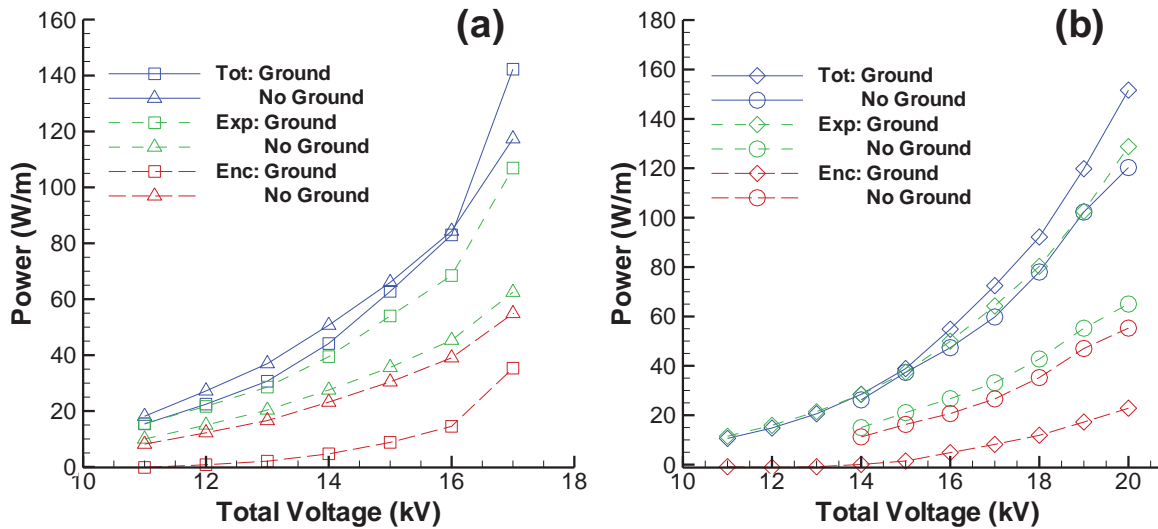

Figure 8. Power distribution in a bi-layer MBPA with and without a middle grounded electrode present. a) L_g = 5 mm and b) L_g = 10 mm.

C. Tri-layer MBPA

A natural extension to the bi-layer MBPA is the tri-layer configuration, where another dielectric layer and powered electrode is added (figure 2c). In the current investigation of the tri-layer MBPA all 4 electrodes are supplied with the same potential. A linear progression in the relative phase angles for the sandwiched electrodes is investigated meaning that β_1 and β_2 equal $\pm 60^o$ and $\pm 120^o$, respectively, while the encapsulated electrode has an 180° phase shift. Again, positive values of β refer to a leading arrangement while negative values are considered lagging.

Results for the measured thrust and consumed power are presented in figure 9 plotted against the total voltage supplied to the actuator. Note that for the tri-layer actuator, the total voltage (as defined above) is identical to that of the bi-layer design. This is the case as well for the tri-layer configuration since the maximum voltage supplied to the device is still the potential difference between the exposed and lower encapsulated electrode due to the fact that all the electrodes are supplied with the same potential only shift temporally.
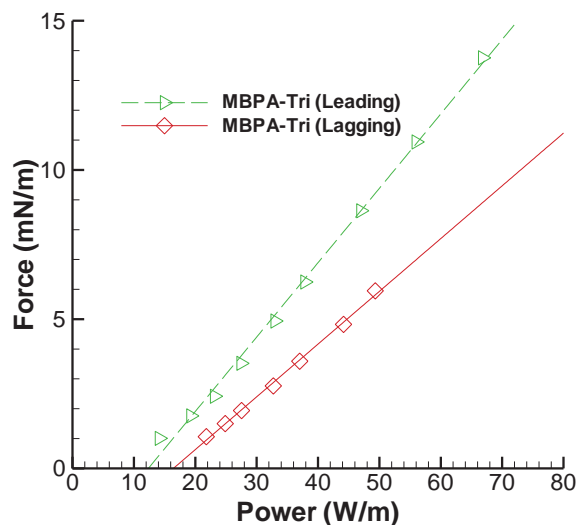
The force measurements reveal that there is a large discrepancy in the produced thrust between a leading and lagging circuit, especially since the consumed power is relatively the same (particularly at low voltages). For example, for a total voltage of 12 kV the leading circuit produced 8.4 mN/m force and consumed 47.2 W/m, while the lagging circuit only produced 3.6 mN/m for 37.8 W/m. This difference results in a ~190% increase in effectiveness (γ) between a leading and lagging configuration. This point is further highlighted in figure 10 which plots the resultant thrust against consumed power. Again, for a given power consumption a leading circuit produces significantly more thrust than that of a lagging configuration.
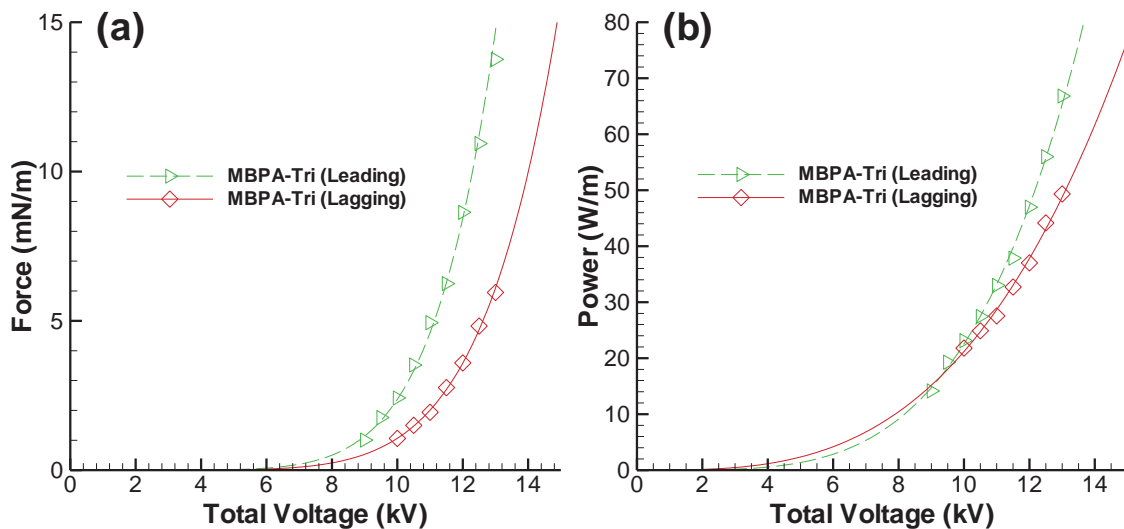
Figure 9. Resultant force (a) and consumed power (b) for a tri-layer MBPA with leading and lagging relative phase angles.

A potential explanation for such a result may be found in the voltage and current waveforms (figure 11). It has been widely documented both experimentally and numerically (sometimes with quite contradicting results) that the plasma behaves quite differently over a single period of the input signal. From figures 11a and 11b one can see that the large ionization spikes in the current signal, which are attributed to micro discharges, occur on different sides on the exposed electrode's voltage waveform depending on the particular lead-lag configuration. For the leading circuit the majority of ionization appears to occur on the forward stroke (in keeping with prior nomenclature[4, 5]) or negative $d\phi/dt$, while ionization appears to take place primarily on the backward stroke for a lagging circuit.

This switching in the apparent primary location of the ionization is a direct result of the phase shifts applied to the sandwiched electrodes in the tri-layer design. Recent work has shown

Figure 10. Induced force plotted against power consumption for leading and lagging relative phase.

that the forward stroke of the waveform contributes signifying more to the total force than that of the backward stroke.[13-16] At face value, this discrepancy between a leading and lagging circuit could seeming be explained by these

7

prior findings. However, to truly confirm this hypothesis one needs to know something about the structure of the discharge since the ionization spikes are only an indication of large scale irregularities in the discharge. At this time no equipment was available to visually capture the plasma discharge with sufficient time resolution such as experiments described in reference 4 or 14.
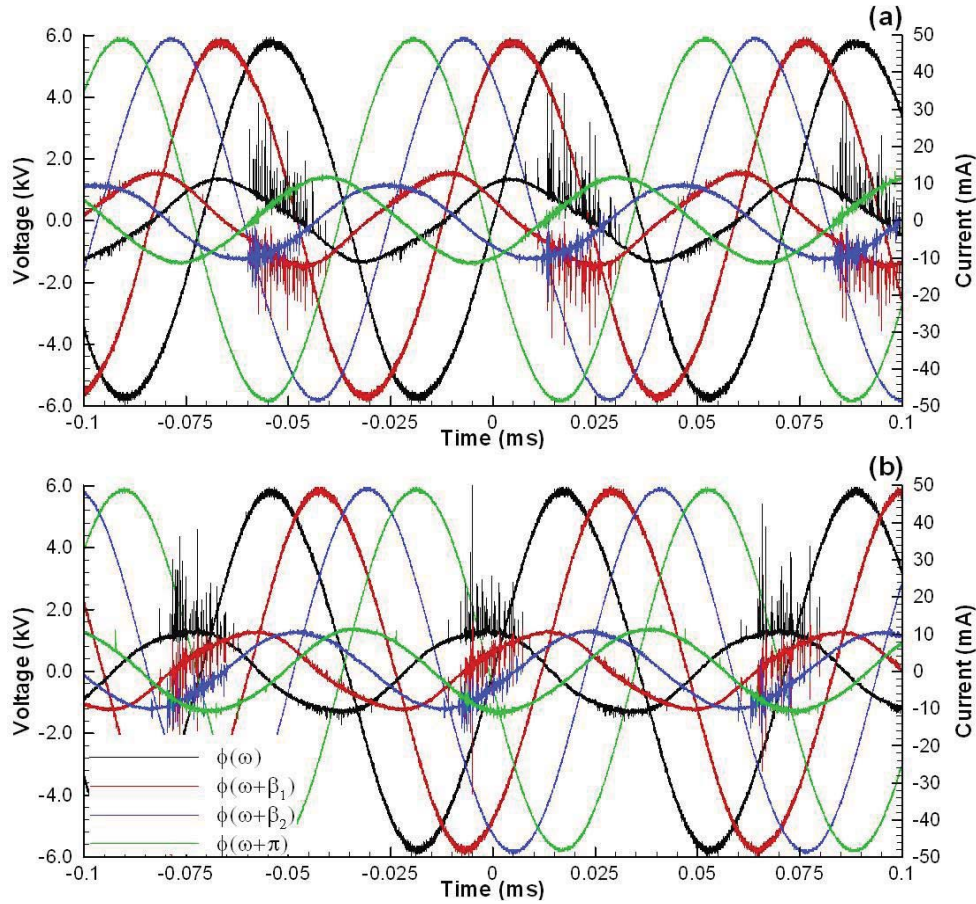

Figure 11. Instantaneous voltage and current waveforms for a leading (a) and lagging (b) tri-layer MBPA. Note that a positive β refers to a leading phase angle while negative values are considered lagging.

D. Comparison of actuator designs

A comparison between a standard actuator, a bi-layer MBPA, and a tri-layer MBPA is shown in figure 12 for both resultant thrust and effectiveness. One can see from the figure that for a constant total voltage and a constant overall thickness of the dielectric, that the standard actuator produces more thrust than the MBPA configurations. These results are consistent with prior preliminary data.[12] Conversely, when one compares the designs on an effectiveness basis (figure 12b) the bi-layer MBPA clearly outperforms the other designs. An increase in effectiveness of ~160% is shown for a bi-layer configuration over the standard actuator. This fact has significant system level design implications.

Although not producing a higher force the bi-layer MBPA provides more force for a given amount of power. This allows one to reduce the size and weight of the required power supply. The design also allows the high voltage to be distributed between multiple electrodes. This then reduces the voltage requirements of an individual power supply; for instead of requiring a 30 kV source one can simply use two 15 kV power supplies. Logic then follows that a decrease in output voltage further reduces the size and weight of the power supply.
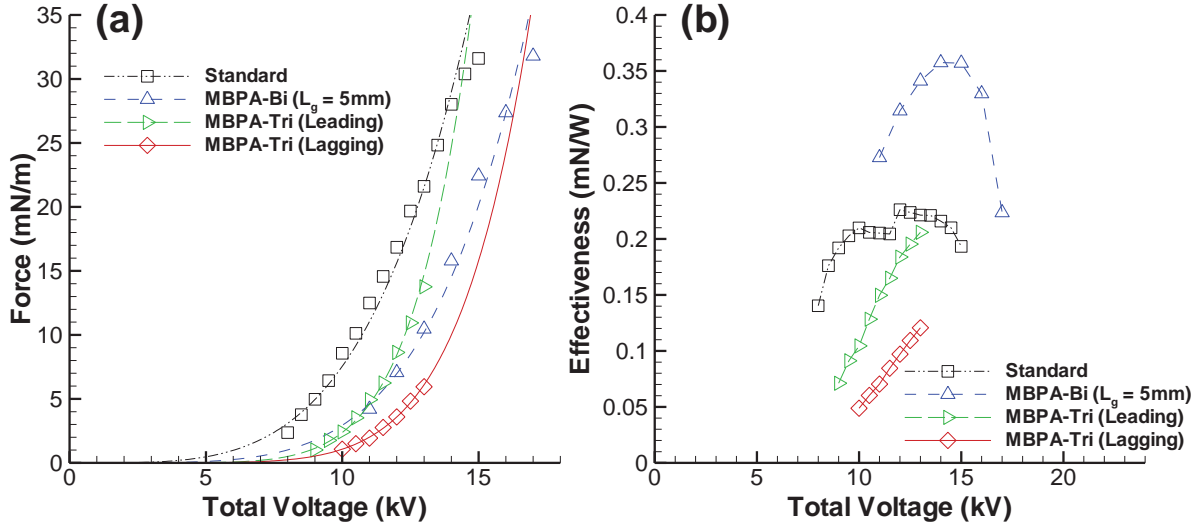
Figure 12. Comparison of actuator configurations: a) force and b) effectiveness.

Questions remain through, what makes the bi-layer more effective than the standard and why the tri-layer design is the least effective? To address the former it was shown above that the total power supplied to a bi-layer MBPA when the middle grounded electrode is present, particularly at low voltages, is primarily consumed by the exposed electrode. As such the current flowing through that branch in the circuit should account for approximately 100% of the total current delivered to the device. Therefore, one may ignore the encapsulated electrode in the bi-layer MBPA and simply compare the instantaneous current waveform of the exposed electrode with that of the standard design (figure 13). When looking at the comparison found in figure 13 one observation stands out in particular. That is, the peak current reached is higher for the standard actuator. Based on this remark it is reasonable to postulate that since Joule heating is proportional to I^2 that the standard actuator is physically heating up more than that of the MBPA, with the waste heat contributing little to the momentum coupling of the surrounding fluid. Although no temperature measurements have been made to date, future tests will be conducted using an IR camera to verify this experimentally.

The second question proposed above about the ineffectiveness of the tri-layer design is a harder one to answer. The simple response would be that this particular geometry chosen was not optimal. It was shown previously for a bi-layer MBPA that a width (L_g) of 10 mm for the middle electrode was not an efficient operating point in terms of force production or effectiveness. For the tri-layer design the total separation length between the exposed and encapsulated electrode was 10 mm (or $2w$ figure 2c). Whether or not such a large separation is the root cause in the poor performance of the tri-layer still needs to be explored and future MBPA designs will address this question by decreasing the width of sandwiched electrodes.
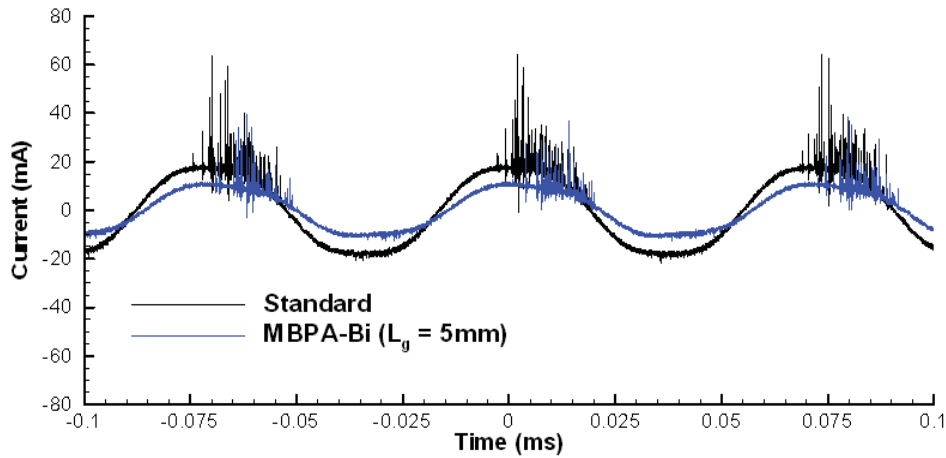
Figure 13. Instantaneous current waveforms for a standard actuator and bi-layer MBPA (exposed/top electrode only) for a total voltage of 13kV.

9

American Institute of Aeronautics and Astronautics

E. Varying dielectric materials

As a starting point to the broad design space of mixed dielectrics, a single combination for a bi-layer MBPA has been investigated. The result of such effort is plotted in figure 14. The bi-layer mixture consists of acrylic and Teflon® which each had a thickness of 1.5 mm (i.e. t = 3mm). The notation "Teflon-Acrylic" shown in figure 14 indicates that Teflon® is the first (or top) dielectric and acrylic is the second (or bottom) dielectric referring to figure 2b. These preliminary results indicate that mixing the dielectrics has little influence on the resultant thrust, with the exception being at high values of total voltage. However, the dielectric constants (ε) for the two materials are 2 and 3 for Teflon® and acrylic, respectively. Such close values could explain why little difference was observed.
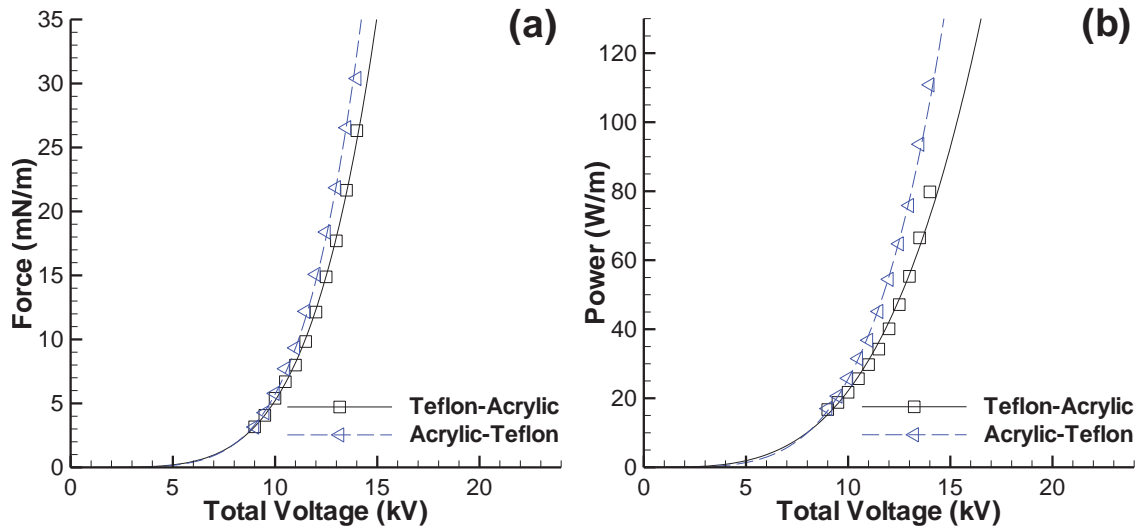

Figure 14. Resultant force (a) and consumed power (b) for a mixed dielectric bi-layer MBPA.

IV. Conclusions

An exploration of the MBPA design space has been carried out. The influence the middle electrodes width has on the performance of a bi-layer MBPA has been ascertained. A width of 5mm was found to be an optimum operating point in terms of effectiveness (ratio of induced force to consumed power). However, based on these findings it was speculated that the middle electrode played no significant role in force production and that by changing its width one was simply varying the relative gap between the exposed and encapsulated electrode. To verify this postulate the middle electrode was removed from the bi-layer configuration and the experiments were repeated. Although, not affecting the induced force or total power consumed the middle electrode was found to play an important role in how the consumed power was disturbed amongst the powered electrodes. When removed, each branch in the bi-layer MBPA circuit contributed roughly equally to the overall power consumption. When the grounded electrode was present, however, the exposed electrode used significantly more power (especially at lower voltages) than the encapsulated electrode. This odd distribution behavior was attributed to the "stepping stone" effect that the grounded electrode creates for the electric field lines when present.

The effect of relative phase angle of the performance of a tri-layer MBPA was explored. A large discrepancy in the resultant force and supplied power was found between a leading and lagging circuit configuration. Although no definitive conclusion was made, it is speculated that the large difference is a result of switching the apparent primary location of ionization from the forward to the backward stroke (referring to the exposed electrode's voltage waveform) for a leading and lagging circuit, respectively.

Additionally, comparisons were made between standard, bi-layer, and tri-layer actuators. In terms of pure force production the standard actuator was the clear winner. When power consumption was taken into account, however, the bi-layer configuration significantly outperformed the other designs. An improvement in effectiveness of ~160% is shown for a bi-layer configuration over the standard actuator. A preliminary investigation of mixing dielectric materials in the bi-layer design was also explored. The results indicated that mixing the dielectrics has little influence on the resultant thrust. This could be attributed, however, to the relatively small difference in the materials' dielectric constant. Future experiments will test largely disparate dielectric materials.

References

[1]Moreau, E., "Airflow control by non-thermal plasma actuators," *J. Phys. D: Applied Physics*, Vol. 40, 2007, pp.605-636.

[2]Abe, T., Takizawa, Y., Sato,S., and Kimura, N.,. "A Parametric Experimental Study for Momentum Transfer by Plasma Actuator." *45th AIAA Aerospace Sciences Meeting and Exhibit*, AIAA Paper 2007-187,Reno, NV, January, 2007.

[3]Roth, J. R. and Dai, X., "Optimization of the Aerodynamic Plasma Actuator as an Electrohydrodynamic (EHD) Electrical Device," *44th AIAA Aerospace Sciences Meeting and Exhibit,* AIAA Paper 2006-1203, Reno, NV, January, 2006.

[4]Enloe, C. L., McLaughlin, T. E., VanDyken, R. D., Kachner, K. D., Jumper, E. J., and Corke T. C., "Mechanisms and Responses of a Single Dielectric Barrier Plasma Actuator: Plasma Morphology," *AIAA Journal,* Vol. 42, No. 3, 2004, pp 589-594.

[5]Enloe, C. L., McLaughlin, T. E., VanDyken, R. D., Kachner, K. D., Jumper, E. J., Corke, T. C., Post, M., and Haddad, O., "Mechanisms and Responses of a Single Dielectric Barrier Plasma Actuator: Geometric Effects," *AIAA Journal,* Vol. 42, No. 3, 2004, pp 595- 604.

[6]Forte, M., Jolibois, J., Pons, J., Moreau, E., Touchard, G., Cazalens, M., "Optimization of a dielectric barrier discharge actuator by stationary and non-stationary measurements of the induced flow velocity: application to flow control," *Exp Fluids*, Vol. 43, 2007, pp 917-928

[7]Hoskinson, A. R., Hershkowitz, N., and Ashpis, D. E., "Force measurements of single and double barrier DBD plasma actuators in quiescent air," *J. Phys. D: Applied Physics*, Vol. 41, 2008.

[8]Opaits, D. F., Zaidi, S. H., Shneider, M. N., Miles, R. B., Likhanskii, A. V., Macheret, S. O., and Ashpis, D., "Improving Thrust by Suppressing Charge Build-up in Pulsed DBD Plasma Actuators," *47th AIAA Aerospace Sciences Meeting Including The New Horizons Forum and Aerospace Exposition*, AIAA Paper 2009-487, Orlando, FL, January, 2009.

[9]Thomas, F. O., Corke, T. C., Iqbal, M., Kozlov, A., and Schatzman, D., "Optimization of Dielectric Barrier Discharge Plasma Actuators for Active Aerodynamic Flow Control," *AIAA Journal,* Vol. 47, No. 9, 2009, pp 2169- 2177.

[10]Corke, T. C., Enloe, C. L., and Wilkinson, S. P., "Dielectric Barrier Discharge Plasma Actuators for Flow Control," *Annual Review of Fluid Mechanics*, Vol. 42, 2010, pp 505–29

[11]Roy, S., "Method and Apparatus for Multibarrier Plasma Actuated High Performance Flow Control," Patent WO 2009/005895, Published Jan 8, 2009 (filed May 2007).

[12]Durscher,R., and Roy, S., "Novel Multi-Barrier Plasma Actuators for Increased Thrust," *48th AIAA Aerospace Sciences Meeting Including the New Horizons Forum and Aerospace Exposition*, AIAA Paper 2010-965, Orlando, FL, January, 2010.

[13]Kim, W., Do, H., Mungal, M. G., and Cappelli, M. A., "On the role of oxygen in dielectric barrier discharge actuation of aerodynamic flows," Applied Physics Letters, Vol. 91, 2007, Article No. 181501

[14]Enloe, C. L., McHarg, M. G., and McLaughlin, T. E., "Time-correlated force production measurements of the dielectric barrier discharge plasma aerodynamic actuator," *Journal of Applied Physics*, Vol. 103, 2008, Article No. 073302.

[15]Enloe, C. L., McHarg, M. G., Font, G.I., and McLaughlin, T. E, "Plasma-induced force and self-induced drag in the dielectric barrier discharge aerodynamic plasma actuator," *47th AIAA Aerospace Sciences Meeting Including The New Horizons Forum and Aerospace Exposition*, AIAA Paper 2009-1622, Orlando, FL, January, 2009.

[16]Orlov, D. M., Font, G. I., and Edelstein, D., "Characterization of Discharge Modes of Plasma Actuators," *AIAA Journal,* Vol. 46, No. 12, 2008, pp 3142-3148.